

University of Wollongong Research Online

Faculty of Engineering and Information
Sciences - Papers: Part A

Faculty of Engineering and Information
Sciences

1-1-2015

Fatigue properties of intact sandstone in pre and post-failure and its implication to vibratory rock cutting

M N. Badge

Csir-Central Institute Of Mining & Fuel Research

Shivakumar Karekal

Centre for Earth Science and Resource Engineering, CSIRO, Australia, skarekal@uow.edu.au

Follow this and additional works at: <https://ro.uow.edu.au/eispapers>



Part of the [Engineering Commons](#), and the [Science and Technology Studies Commons](#)

Recommended Citation

Badge, M N. and Karekal, Shivakumar, "Fatigue properties of intact sandstone in pre and post-failure and its implication to vibratory rock cutting" (2015). *Faculty of Engineering and Information Sciences - Papers: Part A*. 4575.

<https://ro.uow.edu.au/eispapers/4575>

Research Online is the open access institutional repository for the University of Wollongong. For further information contact the UOW Library: research-pubs@uow.edu.au

Fatigue properties of intact sandstone in pre and post-failure and its implication to vibratory rock cutting

Abstract

The pre-and post-failure fatigue properties of intact sandstone subjected to uni-axial cyclical loading in the laboratory is presented with its possible implication to vibratory rock cutting. The fatigue results subjected to sinusoidal, ramp and square waveforms at cyclic loading frequency of 5 Hz and peak amplitude of 0.05 mm is discussed herewith. It is observed that fatigue behaviour is a function of the dynamic energy of the load and the shape of the waveform. From the presented results, the practical significance of the behaviour of rock and rock masses within the excavation systems subjected to cyclic loads, especially in the vibratory rock cutting is put forward. To substantiate the cyclic breaking of rock under vibratory loading condition, a numerical simulation results using discrete element code is presented. Two loading cases were considered. In the first case, the wedge pick was loaded non-cyclically (monotonically), and in the second case it was loaded dynamically under cyclic sinusoidal loading at 50 Hz frequency. A load-deformation curve under monotonic (non-cyclic) loading condition and cyclic loading conditions were examined. The model showed a drop of about 25% in peak strength in the case of cyclically loaded wedge pick compared to monotonic or quasi-static loading of the wedge pick cutting. It is inferred that the vibratory loading has benefits in fracturing rock at relatively lower load compared to conventional loading

Keywords

rock, vibratory, implication, its, failure, post, pre, sandstone, cutting, intact, fatigue, properties

Disciplines

Engineering | Science and Technology Studies

Publication Details

Badge, M. N. & Karekal, S. (2015). Fatigue properties of intact sandstone in pre and post-failure and its implication to vibratory rock cutting. *ISRM (India) Journal*, 4 (1), 22-27.

FATIGUE PROPERTIES OF INTACT SANDSTONE IN PRE AND POST-FAILURE AND ITS IMPLICATION TO VIBRATORY ROCK CUTTING

M.N. Bagde

CSIR-Central Institute of Mining & Fuel Research, Regional Center, Nagpur, India

S. Karekal

Centre for Earth Science and Resource Engineering, CSIRO, Australia

ABSTRACT

The pre- and post- failure fatigue properties of intact sandstone subjected to uni-axial cyclical loading in the laboratory is presented with its possible implication to vibratory rock cutting. The fatigue results subjected to sinusoidal, ramp and square waveforms at cyclic loading frequency of 5 Hz and peak amplitude of 0.05 mm is discussed herewith. It is observed that fatigue behaviour is a function of the dynamic energy of the load and the shape of the waveform. From the presented results, the practical significance of the behaviour of rock and rock masses within the excavation systems subjected to cyclic loads, especially in the vibratory rock cutting is put forward. To substantiate the cyclic breaking of rock under vibratory loading condition, a numerical simulation results using discrete element code is presented. Two loading cases were considered. In the first case, the wedge pick was loaded non-cyclically (monotonically), and in the second case it was loaded dynamically under cyclic sinusoidal loading at 50 Hz frequency. A load-deformation curve under monotonic (non-cyclic) loading condition and cyclic loading conditions were examined. The model showed a drop of about 25% in peak strength in the case of cyclically loaded wedge pick compared to monotonic or quasi-static loading of the wedge pick cutting. It is inferred that the vibratory loading has benefits in fracturing rock at relatively lower load compared to conventional loading.

1. INTRODUCTION

The understanding how dynamic loading influence rock failure and its behavior has a great significance in excavation systems prone to extreme rock-burst loading, drilling, crushing, blasting and vibratory rock cutting etc.; however, there is almost rare literature on this. It is well reported in the literature that intact and failed models of jointed rock are extremely susceptible to cyclic fatigue failure. For the detailed review and studies on the subject refer to various publications^[1,2,3,4,5,6]. In cited various publications, fatigue behaviour of sandstone, siltstone and conglomerate rocks obtained from the rock-burst prone Ostrava-Karvina coalfield is presented. The significance of low-load frequency and high amplitude in fracturing, micro-fracturing and degradation of various rock properties in cyclic loading is discussed in those publications. The results presented therein were corroborated with the rock burst problem and mitigation of the same. However, here the findings reported earlier were attempted to corroborate with its implications to vibratory rock cutting. As discussed in one of the paper^[4] fracture and fragmentation of sandstone rock was found to affect significantly at low loading frequency when compared to higher frequency and it was suggested that

the most efficient method of rock cutting, excavation, fragmentation and crushing could be low-speed loading. The effect of loading waveform on fatigue properties of the intact rock in pre-failure state are discussed in^[5], while, post-failure properties are reported in^[6] and discussed with relation to seismic rock burst conditions. However, in the present paper, the reported earlier findings will be related to vibratory rock cutting with its significance and importance in rock cutting. Here, an attempt has been made to corroborate fatigue behaviour of the rock with its applications to vibratory rock cutting, its significance and importance in rock cutting with results obtained from the numerical simulation using discrete element modelling.

2. TEST EQUIPMENT AND SCHEME

The details of the tested rock, equipment and test scheme in brief is provided in the following. For the detailed explanation refer to^[5,6]. The rock samples were obtained from the rock burst prone Darkov coal mine in the Ostrava-Karvina coal basin in the Czech Republic. The samples were of 1:1 diameter to length ratio with average diameter of 47.5 mm. Samples were prepared and tested according to ISRM testing procedure and guidelines^[7].

The testing equipment was MTS-816 rock test system. The details about the rock types, testing equipment, test scheme and waveform types and their characteristics can be found elsewhere^[5,6]. The tests were conducted with axial displacement controlling loading system and the dynamic load was specified as a sine, ramp and square cyclic compressive respectively for a given set of test conditions. The illustration of different nomenclatures associated with cyclic loading is provided elsewhere^[5,6]. The illustration of real loading condition on time-displacement curve throughout the uniaxial cyclic loading test is given in Fig. 1.

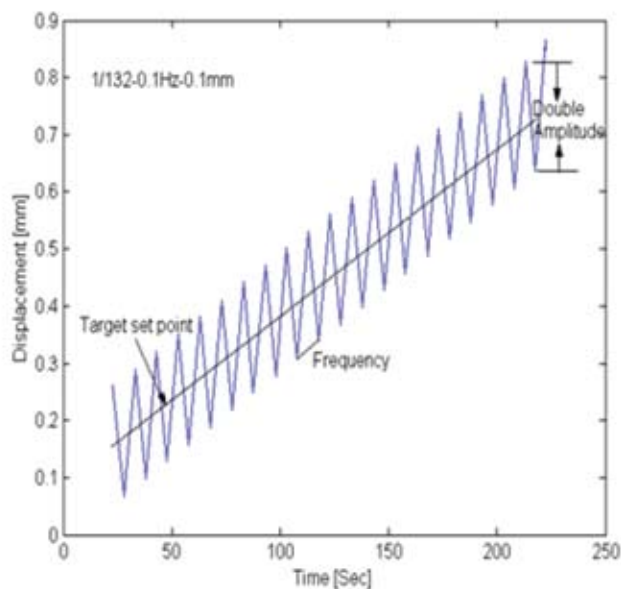


Fig. 1 : Time-displacement curve illustrating uniaxial dynamic cyclic loading condition (example for 0.1 Hz frequency and 0.1 mm amplitude)

The shape of a waveform determines the loading/unloading rate, the rate of change in the loading/unloading rate, and the residence period at the peak stress. The illustration of three waveforms with their characteristics can be found in detailed in^[5,6]. It is well reported and established in rock mechanics that loading rate strongly influences the rock behaviour. The numerous studies is being reported in the literature where strain rate or loading rate effect on various rock properties is discussed. The detailed discussion about the maximum loading rate in a waveform and its influence on fatigue rock behaviour in uniaxial cyclic dynamic loading conditions is discussed in the following with their possible applications to vibratory rock cutting.

3. EVALUATION OF ROCK PROPERTIES UNDER CYCLIC LOADING

The data from the cyclic loading tests were analyzed to obtain various fatigue properties of the tested rock. An illustration of stress and modulus computation from peak-

valley data using a computer programme is given in Fig. 2. For the detailed explanation refer to^[5,6].

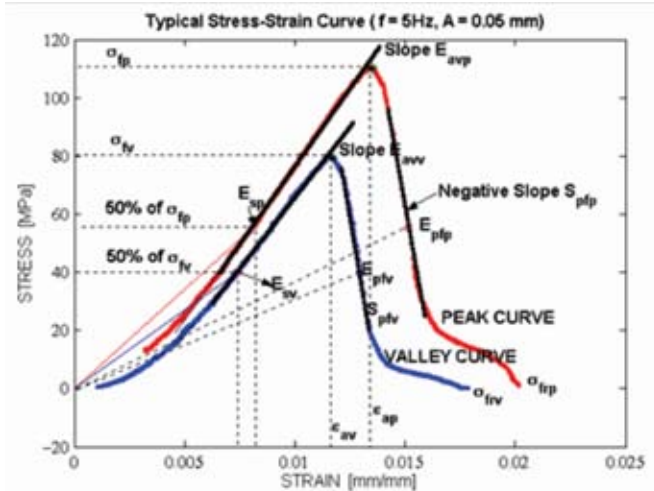


Fig. 2 : Typical stress-strain curve with illustrating calculation of various rock properties in pre- and post-failure curves from peak-valley data in uni-axial cyclic loading condition

4. EXPERIMENTAL RESULTS AND DISCUSSION

Tests were conducted to study the effect of waveform on the cyclic fatigue behaviour of sandstone rock in uniaxial cyclic loading conditions. The sinusoidal, ramp and square waveforms were used with a load frequency of 5 Hz and amplitude of 0.05 mm. The results presented and discussion made herewith are based on the average results. On an average three samples were tested for individual testing conditions.

The dynamic fatigue strength obtained was higher in the case of ramp loading waveform compared to that of sinusoidal and square (Fig. 3). The post-failure negative slope (Fig. 4) found to be higher in the case of ramp, followed by sinusoidal and least in the case of square waveform. The least post-failure negative slope in the case of square waveform suggests that under such condition rock would fail in more brittle and or violent manner due to the residence period (means constant load amplitude during residence period) and high loading rate when compared to others.

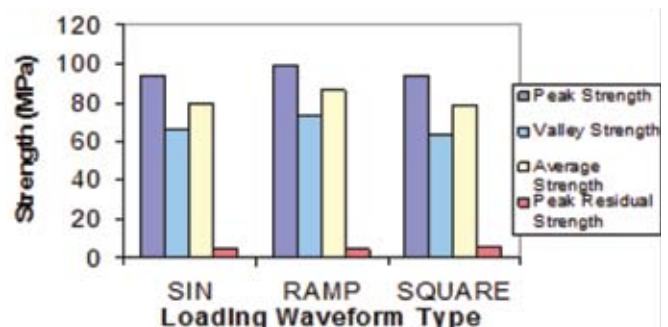


Fig. 3 : Strength with loading waveforms^[6]

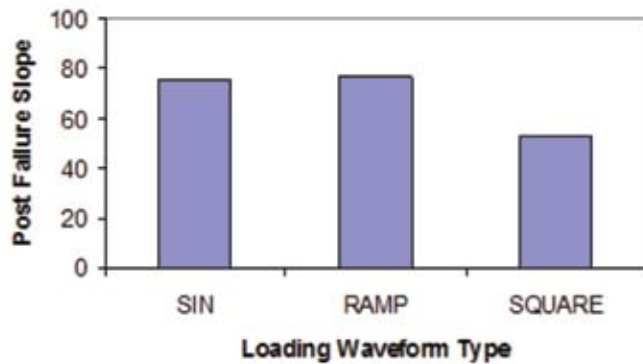


Fig. 4 : Post failure slope with loading waveforms^[6]

Also, when compared results presented in Fig. 5, the average dynamic Young's modulus (E_{avd}) was higher in the case of ramp than other two waveforms considered. In the case of sinusoidal, it was found to be least. In the case of secant modulus, it was least in the square and higher in the case of the sinusoidal waveform. Also, reversible modulus was found to be higher in the case of ramp, followed by sinusoidal and least in the case of square waveforms. The post-failure modulus found to be the least in the case of square waveform. When compared all those presented results as above, it is concluded that the damage accumulated most rapidly under the square waveforms compared to others. The maximum loading rate in a waveform found to strongly influence the damage accumulation in rock and it is the square waveform-the most damaging one from the presented results. Also, the larger disparity between the secant and the Young's modulus values suggest the greater initial crack density in the case of square waveform. From the presented results, it is concluded that residence period and thus constant loading amplitude during residence time in the case of square waveform compared to others helps in better fragmentaion and micro-fracturing of the rock resulting in degradation of the most of the fatigue rock properties.

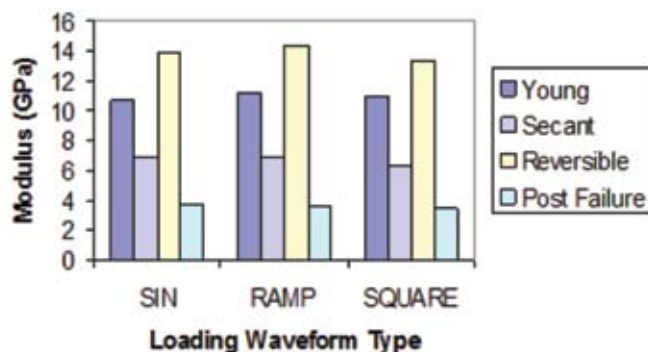


Fig. 5 : Modulus with loading waveforms^[6]

The dynamic energy (D_e) utilized to cause rock failure was found least in the case of ramp waveform compared

to that sinusoidal and square (Fig.6). In the case of square waveforms, it was found that dynamic energy requirement was more to cause failure of the rock samples. From this, it could be concluded that a ramp waveform is the least damaging of those considered. The damage accumulated most rapidly under square waveforms with a high dynamic energy requirement and followed by sinusoidal and ramp waveforms. These results demonstrate that it is the loading rate or loading waveform that mainly contributes to the damage in rock specimens. Thus, it is inferred that the higher the workdone per cycle during low cycle fatigue tests, the shorter the time to failure will be. It means that the higher amplitude and or constant amplitude for long-residence period and low-frequency is of the great significance in cyclic loading conditions which will help in better rock fragmentaion and fracturing and early failure means low-fatigue life. It is found that crack propagation is better allowed to occur in the case of low-loading frequency than the higher one. The loading amplitude is found to have significant influence on the rock fatigue behaviour and degradation of the rock properties.

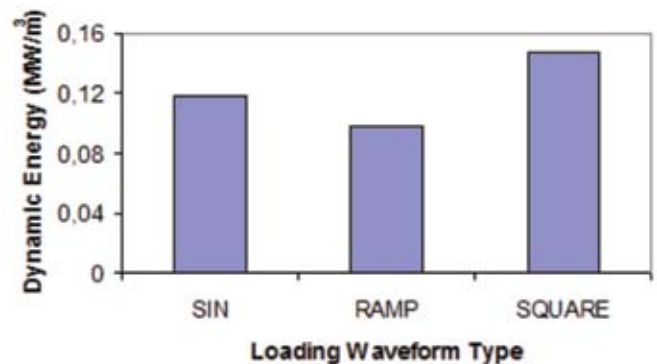


Fig. 6 : Dynamic energy with loading waveforms^[5]

This study focused on investigating the effects that waveform and amplitude have on the dynamic cyclic fatigue behaviour of intact sandstone rock. Based on the work presented, the following inferences are made:

Fatigue behaviour of the rock due to uniaxial cyclic compression is a function of the shape of waveform and the workdone by the load. The damage accumulates most rapidly under the square waveforms with a high energy requirement. The ramp waveform is less damaging than either square or sinusoidal waveforms. The ramp waveform found to be uniform in loading and unloading with less dynamic energy requirement to cause failure in the rock samples for a given loading frequency and amplitude. The loading waveforms strongly influences the damage accumulation (accumulated deformation) under cyclic loading conditions. It is found that the maximum loading rate in a waveform strongly influences

the damage accumulation in rock. It is found that type of loading waveform affects the various pre- and post-failure rock properties presented here in dynamic uniaxial cyclic loading conditions. The possible applications of the presented fatigue behaviour results is discussed with reference to vibratory rock cutting and corroborated with the findings from the discrete element simulation results in the following.

5. DISCRETE ELEMENT SIMULATION OF VIBRATORY ROCK CUTTING

To substantiate the new technique of breaking hard rock under variable amplitude cyclic loading and unloading (or under vibratory loading condition), a numerical simulation using discrete element code (Universal Distinct Element Code, UDEC) was used.

The numerical methods are becoming more attractive and popular now days for modeling the complex rock-tool interaction processes because idealized analytical methods with simplified assumptions do not fully capture the failure process. The various continuum numerical codes such as FEM, BEM and FLAC have been used to understand the rock-tool interaction process. These models have been developed either through incorporation of failure theories or through the use of fracture mechanics with pre-existing cracks^[8,9,10]. The Discrete Element Method (DEM), particularly Particle Flow Code (PFC), has been used to simulate the failure process of rock by mechanical indentation^[11].

The general process of wedge cutting using discrete element code is illustrated in Fig.7.

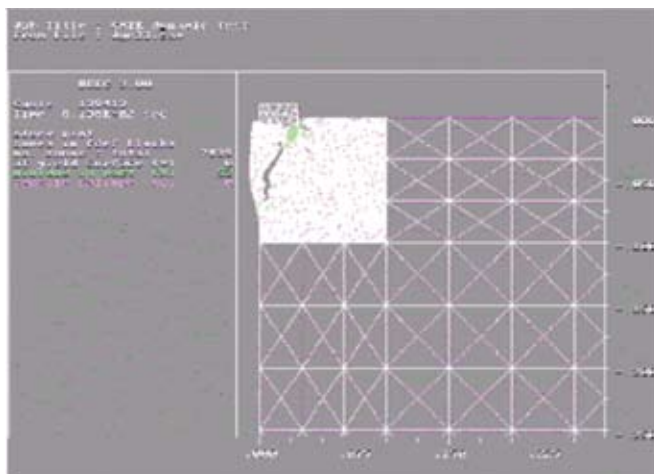


Fig. 7 : Crushing and fracturing in wedge pick cutting of simulated material^[12]

When a pick is pressed against the rock at a certain edge distance, a plastic zone (crushing) forms beneath the indenter, and a distinct crack emanates from the crushed zone and extends laterally to its free surface forming a chip (Fig.7). The DEM seems to capture both

the crushing and crack development processes observed in experimental rock cutting.

In the simulations carried out^[12], two loading cases were considered. In the first case, the wedge indenter was loaded non-cyclically (monotonically), and in the second case was loaded under variable amplitude at 50 Hz frequency (Fig. 8).

The rock block having dimensions of 1m depth and 1m width was used for the simulation. A square of 100 mm by 100 mm of the inner region (Fig. 7) was further subdivided into smaller jointed blocks to treat this region as a discontinuum, and to understand the fracturing process better^[12]. Viscous boundary conditions were applied along the left boundary to prevent failure due to the reflection of a wave from the boundary. A constant velocity boundary condition of 100 mm/s was applied along the top of the wedge pick (under quasi-static loading). In another case, in order to investigate the effect of vibratory motion of the cutter on the force-penetration curve, the cutter/indenter was vibrated at 50 Hz, with amplitude of 1.5 mm. In all the cases, the cutter was allowed to move in Y – direction (vertically down) and its movement in X direction was restricted.

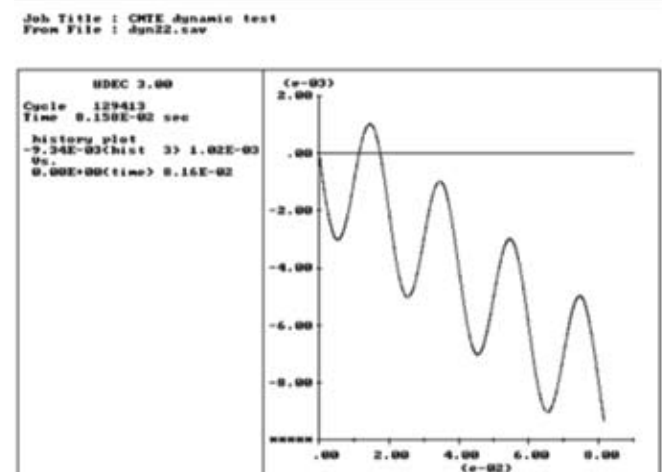


Fig. 8 : Variable amplitude cyclic displacement boundary condition with time

The Mohr-Coulomb failure criterion with a strain softening constitutive model was adopted for deformable blocks. For joints, a Coulomb joint slip failure constitutive model was chosen as it allows understanding of the general indentation mechanisms. For comparison of force-penetration curves in cyclic and non-cyclic motion of the cutter, a continuously yielding joint model was adopted^[12]. In all the cases, a friction angle of 10° was chosen between the indenter and the rock. Also the material properties were kept same for all the simulations. Figs. 9 and 10 show the force-penetration curves under these loading conditions.

These simulation results^[12] show that a peak force of 13.2 kN was attained before failure was achieved during monotonic (non-cyclic) loading. However, with cyclic loading the peak force achieved was reduced to 9.93 kN (about a 25% drop). It can be inferred from the simulation results that variable amplitude cyclic loading requires relatively less force to fracture compared to non-cyclic loading in the configuration considered. From the studies where fatigue behavior of the rock is discussed in cyclic loading also inferred that low-loading frequency with higher amplitude or constant loading amplitude during residence period in the case of square waveform was found to be most damaging. It is also observed that crack propagation will be better in the case of low-loading frequency and damage accumulation will be more in the case of higher amplitude.

Job Title : CMTS dynamic test
From File : jk99.sav

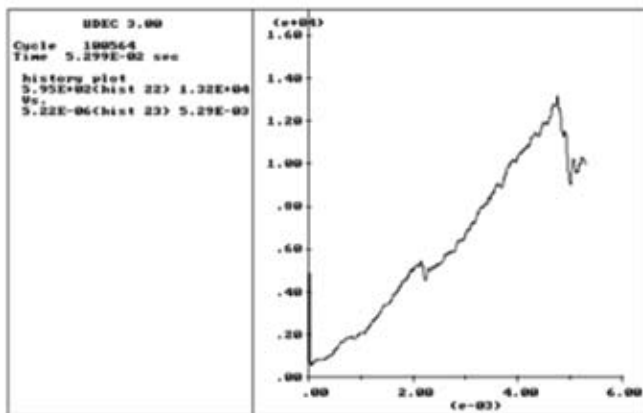


Fig. 9 : Load-Displacement curve in non-cyclic loading

Job Title : CMTS dynamic test
From File : jk99.sav

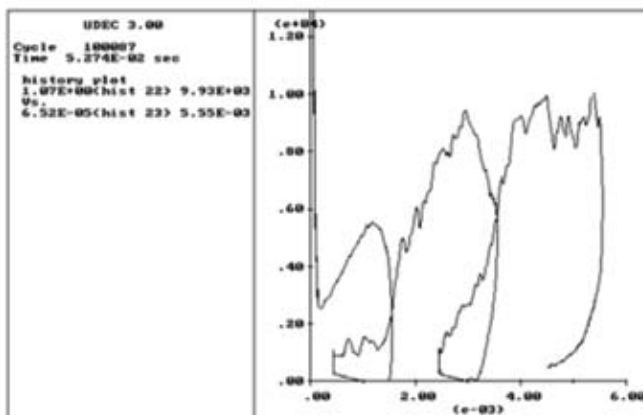


Fig. 10 : Load-Displacement curve in variable amplitude cyclic loading

Further work is needed before findings of the present study can be applied in a quantitative sense, and more focus is needed on the experimental program on the vibratory rock cutting and verification through model simulation with appropriate constitutive equations.

ACKNOWLEDGEMENTS

The views expressed in this paper are of those authors and not necessarily of the institute, to which they belong.

REFERENCES

1. Bagde M.N. and Petros V. 2009. Fatigue and dynamic energy behavior of the rock subjected to cyclical loading. *Int. J. Rock Mechanics & Mining Sciences*, 46, 200-209.
2. Bagde M.N. and Petros V. 2005. Fatigue properties of intact sandstone samples subjected to dynamic uniaxial cyclical loading. *Int. J. Rock Mechanics & Mining Sciences*, 42, 237-250.
3. Bagde M.N. and Petros V. 2005. The effect of machine behaviour and mechanical properties of intact sandstone under static and dynamic uniaxial cyclical loading. *Rock Mechanics & Rock Engineering*, 38 (1), 59-67.
4. Bagde M.N. 2010. Fracture and fragmentation of rock subjected to uniaxial cyclical loading. In *Proc. GeoFlorida 2010: Advances in Analysis, Modeling, & Design (GSP 199)*, Reston VA (Ed), USA:ASCE,2010:214-223. Conf.Proc. doi:10.1061/41095(365)18. <http://site.elibrary.com/lib/nwvu/Doc?id=10475974&pg=260>.
5. Bagde M.N. and Petros V. 2005. Waveform effect on fatigue properties of intact sandstone in uniaxial cyclical loading. *Rock Mechanics & Rock Engineering*, 38 (3), 169-196.
6. Bagde M.N., Petros V. 2009. Waveform effect on pre- and post-failure fatigue properties of sandstone. In *7th Int. Symp. on Rockburst and Seismicity in Mines (RaSiM7) : Controlling Seismic Hazard and Sustainable Development of Deep Mines*, Dalian, China, 21-23 August 2009, Tang CA (Ed), Rinton Press, 407-414.
7. Fairhurst, C.E. and Hudson, J.A. 1999. Draft suggested method for the complete stress-strain curve for intact rock in uniaxial compression. In *International Society for Rock Mechanics Commission on Testing Methods*, Fairhurst, C. E. and Hudson, J. A. (Co-ordinators), *Int. J. Rock Mech. Min. Sci.* 36, 279-289.
8. Wang J.K and Lehnhoff T.F., 1976. Bit penetration into rock – a finite element study. *Int. J. Rock Mech Min Sci*, 13(11-6).

9. Korinets A.R. and Alehossein H. 1996. DIANA modeling of a rolling disc cutter and rock indentation. In Aubertin, et al. (eds). Rock mechanics: p647. Rotterdam: Balkema.
10. Tan C.A., Kou S.Q and Lindqvist P. 1996. Simulation of rock fragmentation by indenters using DDM and fracture mechanics. In Aubertin, et al. (eds). Rock mechanics: p685. Rotterdam: Balkema.
11. Huang H., Detournay E. and Bellier B. 1999. Discrete Elem Korinets A.R. and Alehossein H. 1996. DIANA modeling of a rolling disc cutter and rock indentation. In Aubertin, et al. (eds). Rock mechanics: p647. Rotterdam: Balkema.
12. Karekal, S. 2001. Investigation of rock indentation process, 9th Annual JKMRC conference, Brisbane, Australia. PP. 107-138

BIOGRAPHICAL DETAILS OF THE AUTHORS



Dr. Manoj Namdeo Bagde graduated in Mining Engineering with first division in the year 1993 from Visvesvaraya Regional College of Engineering, Nagpur (presently known as VNIT). He has obtained his M. Tech in Rock Mechanics in the year 1994 from Indian Institute of Technology, Delhi. He was awarded Ph. D. degree in Mining Geomechanics in June 2004 by VSB-Technical University, Ostrava, Czech Republic under Czech Govt. Scholarship. He has worked as a visiting fellow during 2010- 2011 at McGill University, Canada under BOYSCAST Fellowship of DST, GOI. He has joined Central Institute of Mining and Fuel Research in the year 1996 and presently working as Principal Scientist in the area of Rock Mechanics and Mining Engineering at CIMFR Regional Center, Nagpur. His area of interest includes Rock Mechanics and Ground

Control, Mining Methods and Ground Support in Mines, Tunnels and Caverns, Backfill failure in hard rock metal mines etc. He has made a significant contribution by publishing technical R & D articles in well known Journals of International repute. Till date he has to his credit 7 International Publications, 6 in National Journals and more than 40 publications in International & National Conferences and Seminars etc. He has visited Australia, Canada, Hong Kong and Czech Republic and presented technical papers at different worldwide forums.



Dr. Shivakumar Karekal (Project Leader, CSIRO, Australia) has Bachelor and Master degrees in Mining Engineering and PhD in Mining, Mineral and Materials from the University of Queensland. He has 23 years of research experience worked at several research organizations such as National Institute of Rock Mechanics (India), Centre for Mining Technology and Equipment (CMTE), Australia, Lecturer, Division of Mining, Mineral and Materials, University of Queensland, and CRC Mining. He was associated with world renowned research organizations such as Norwegian Geotechnical Institute (NGI), Norway, National Institute of Advanced Industrial Science and Technology (AIST), Japan, Sustainable Mining Institute (SMI) and JKMRC, Australia. He was a nodal coordinator for Mining Education Australia (MEA) geo-mechanics courses and a national coordinator for drilling and blasting curriculum for Mining Education Australia (MEA) administered by the Mineral Council of Australia (MCA). He is currently with CSIRO. He has executed several national and international projects and has patents in advanced cutting technology in USA, Germany, South Africa, and Australia. His main interest is the application of advanced and innovative technologies for solving mining industry problems.

DESIGN OF LINING FOR A MINE SHAFT AND DECLINE USING NUMERICAL MODELLING TECHNIQUES

Islavath Sreenivasa Rao

Department of Mining Engineering, University of Engineering (KU), Kothagudem, India

Debasis Deb and Sujeet Bharti

Department of Mining Engineering, IIT Kharagpur, India

ABSTRACT

A chromite ore body located in eastern India is to be extracted by sub-level open stoping method. A vertical circular shaft and a decline are required to be developed for transporting man, material and air. It is decided that the shaft and the portal of the decline will be located in the footwall side of the ore body. The top most cross-cut from the decline will contact the ore body at about 170 mRL. This study has been conducted to evaluate the engineering properties of lining material and its thickness for the proposed shaft and decline geometry. In order to perform such tasks, borehole rock samples are tested to estimate the engineering parameters of the country rocks and ore body. Apart from that rock mass rating (RMR) and geological strength index (GSI) of rocks are also determined. Two dimensional numerical modelling techniques have been employed to estimate the stress and displacement distributions around the decline and shaft. This paper presents the methodology and results of this study and demonstrates the efficacy of numerical modelling technique in stability analysis of shaft and decline.

INTRODUCTION

Out of total reserves in India, 95% of chromite occurs in Orissa, and it has wide usage in chemical and metallurgical industries. The chromite deposit in study extends 290 m in strike length with an average width of 20 m. The top portion of the deposit is located about 30 m below the surface and extends vertically upto 200 m. The dip angle of the ore body is 100 degree with the horizontal or 800 degree with the vertical. Country rocks of chromite deposit are weathered serpentinite, serpentinite, quartzite and pyroxenite. A quartzite hill exists on the surface towards the dip side of the ore body. The bottom most RL of the surface is 210 mRL.

It is proposed that the chromite ore body will be extracted by sub-level open stoping method with late filling, if required. For this purpose, a vertical circular shaft and a decline need to be developed to access the ore body. The shaft will be located in the footwall side of the ore body. The portal of the decline will also be located in the footwall side of the ore body. The top most cross-cut from the decline will contact the ore body at 170 mRL. This study is required to be conducted to determine suitable thickness of lining of mine shaft and decline and safe location of the shaft. In order to perform such tasks, borehole rock

samples have been tested to estimate the engineering parameters of the country rocks and ore body. Rock Mass Rating (RMR) and Geological Strength Index (GSI) have also been estimated for the same. Two dimensional numerical modelling techniques have been employed to estimate the stress and displacement distributions in the pillars, walls of the stopes, decline and shaft.

OBJECTIVE OF THE STUDY

This study has two main objectives:

- Determination of geotechnical and rock parameters of hanging wall, footwall and ore body of the chromite deposit to use as input to the numerical modelling software.
- Design and stability analysis of the mine shaft and decline using numerical modelling techniques. The method of stoping is 'sub-level open stoping method with late filling, if required'.

GEOTECHNICAL STUDY AND LABORATORY TESTS OF ROCKS

Rock Quality Designation (RQD), Rock Mass Rating (RMR) and Density of rocks (γ)

RQD, RMR and density of ore body and the country rock is determined. RQD varies from 56.81 to 83.65 as listed in Table 1.

Table 1 : RQD RMR of different type of rocks

Rock Type	W.Serpentinite	Serpentinite	Chromite	Pyroxenite	Quartzite
RQD (%)	56.81	83.65	75.41	78.37	63.66
RMR	47	71	75	74	76
Density (kg/m ³)	2745	2745	3537.9	2350	3000

RMR of weathered serpentinite is about 47 and that of all other rocks are above 70. Hence, rocks are found to be competent at greater depth.

Mechanical Parameters of Core Samples

The rock core samples collected from the mine site were cut and polished to the size recommended by the International Society of Rock Mechanics (ISRM). The length to diameter ratio of the uni-axial compressive strength and the tensile strength are 2.5 to 3.0 and 0.5 respectively. The UCS, tensile strength, modulus of elasticity and Poisson's ratio of the rock samples are determined in the laboratory to use as input to the numerical model and are listed in Tables 2 and 3.

Figures 1a and 1b show the sample under uni-axial compression test and tension test. Figure 1c shows the stress-strain behaviour of the chromite samples tested in the laboratory. These figures depict both axial and lateral strains with load increments. It may be noted that the axial strain is considered to be compressive (+ve) while lateral strains are tensile (-ve).

The values obtained from the test are an estimate of the 'Intact Rock Material', whereas, the larger rock mass in situ contains local cracks, fractures and discontinuities, which reduce the strength of the rock mass considerably. Hence, to incorporate this reduction in the rock strength, the rock properties were modified, according to the following equations (Marinos and Hoek, 2000):

$$\sigma_{cm} = (0.003m_i^{0.8})\sigma_{ci}(1.029 + 0.025e^{-0.1m_i})^{GSI} \quad \dots(1)$$

It is found that elastic modulus mostly varies linearly with UCS and hence, deformation modulus is also determined

using equation (1) by replacing UCS by elastic modulus of intact rock.

Again, considering the unforeseen events such as water conditions, local joints and fractures, elastic modulus of rock mass (E_c) is further reduced to 80% as

$$E_{cm} = 0.8E_c \quad \dots(2)$$

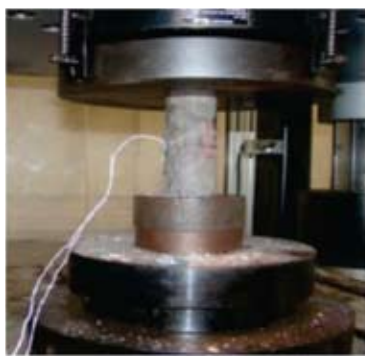
Here, m_i = the Hoek-Brown parameter of intact rock, σ_{ci} = uniaxial compressive strength (Intact rock core), σ_{cm} = uniaxial compressive strength (rock mass), E_{ci} = elastic modulus (Intact rock core), E_c = elastic modulus (rock mass), and E_{cm} = elastic modulus (reduced by 80%). In this study, Poisson's ratio (ν) of intact rock and that of rock mass is kept the same.

NUMERICAL MODELLING FOR DESIGN OF THE MINE SHAFT AND DECLINE

The Finite Element Method

Finite element method is an effective tool for the analysis of mechanical and structural components of machinery. This method is amenable to systematic computer programming and offers a scope for application to a wide range of problems for analysis. This method is now adopted in almost all branches of engineering where complex structures, fluid dynamics problems, mine and tunnel structures and similar problems are addressed (Bathe, K. J., 2007).

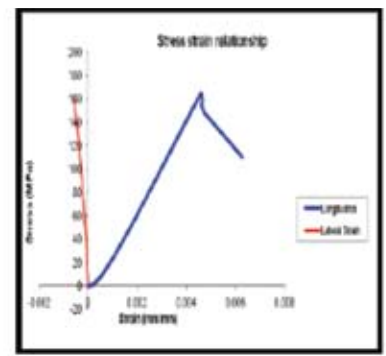
The basic concept in this approach is that a body or structure can be divided into a finite number of smaller units of finite dimensions called 'elements'. The original body or structure is then considered as an assemblage of these elements connected at finite number of joints called



(a) Uni-axial compression test



(b) Tension test



(c) Stress-strain relationship curve

Fig. 1 : Testing of mechanical properties of rocks

Table 2 : UCS and Tenile strength of different rocks

Rock type	W. Serpentinite	Serpentinite	Chromite	Pyroxenite	Quartzite
Avg. UCS (MPa)	132	152.56	113.18	115	110
Avg. (MPa)	4.05	11.82	10.33	3.2	3.5

'nodes' or 'nodal points'. The properties of these elements are formulated and combined to obtain the solution for the entire body or structure. The global system of equations is developed as follows (Deb, 2010):

$$\{F\} = [K]\{q\} \quad \dots(3)$$

Where, $\{F\}$ = global force vector, i.e. forces in each node,

$[K]$ = global stiffness matrix based on material properties,

$\{q\}$ = displacement vector containing each node.

Necessary (essential) boundary conditions in terms of displacements at some selected nodes are applied before solving this system of equations.

Two Dimensional Model

Two 2D-finite element models have been developed to analyze the stress distribution around the decline, the stope and the shaft area and also have been estimated the plastic zone around these three openings. The primary motivation of analyzing in 2D is to determine the failure zone around the decline and the shaft. All 2D models are analysed considering Drucker-Prager materials in plane strain conditions. It means that rock mass is allowed to yield based on its strength and the developed plastic strain intensity has been observed around the excavations (Deb De tal., 2008). The 2D models are described as follows:

- (I) Vertical section comprises host rock, ore body, drives and the decline.

- (II) Horizontal section comprises host rock, ore body and the shaft.

Finite Element Models - 2D (Vertical Section)

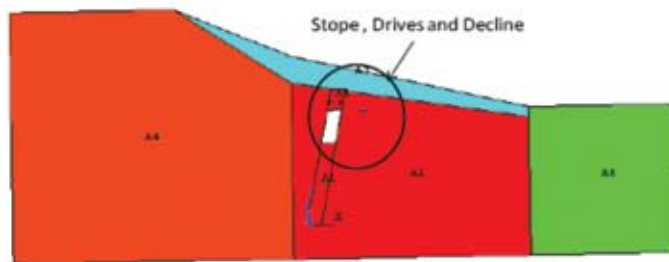
The vertical section of the 2D model is comprised of host rock, ore body and the decline. Vertical section is taken at 165 m away from the boundary of the adjacent mine. Figures 2a and 2b show the excavation model of vertical section which consists of stope, decline and surrounding rock. The in-situ model consists of in-situ ore body with host rock.

Material Properties

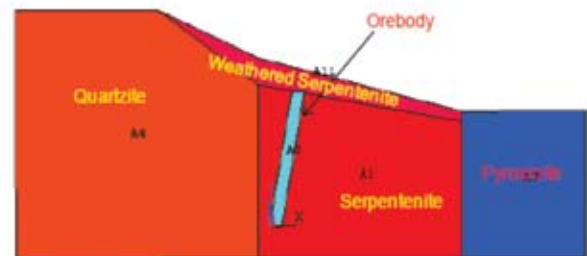
Rock mass properties of these models have been further reduced to simulate more jointed rock mass conditions. Table 3 lists the rock and rock mass properties those are used for finite element modelling for all 2D models. It can be easily seen that compressive strength of rock mass of each rock type is considered at the lower side to incorporate jointed rock mass with few centimetre spacing, weathered and watery conditions.

Generation of Finite Element Meshed Models

The meshing of the excavation model produced an average of around 3,715 six-noded triangular elements and around 7,538 nodes (Figure 3a). Little variations are noted in node counts with in-situ model geometries. Figure 3a shows the meshed model of vertical section of excavation model. In general, finer mesh is developed around the stope, the drives and the decline zones. In those zones, finer mesh is required for better evaluation of displacements, stresses and strains. Coarser mesh is developed in the rock-body away from the mining-affected zones.

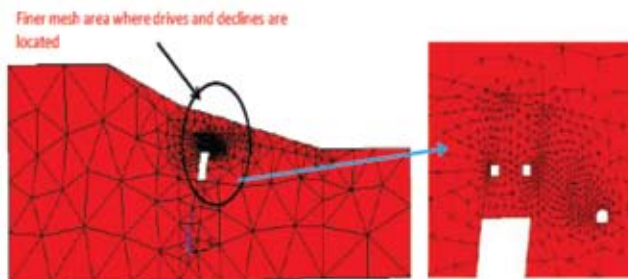


2(a) Vertical section of excavation model

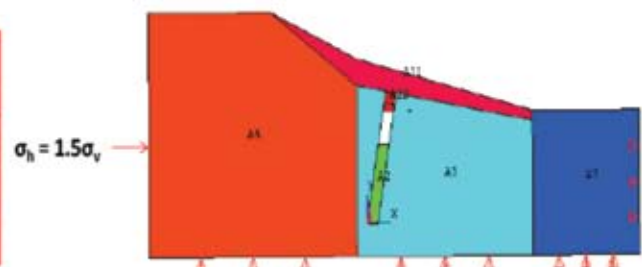


2(b) Vertical section of in-situ model

Fig. : 2a and 2b



3(a) Meshed model



3(b) Boundary conditions are applied

Fig. : 3a and 3b

Table 3 : Material properties used in the models

Rock or Material	Modulus of Elasticity (MPa)	Poisson's Ratio (ν)	Density (kg/m ³)	Compressive Strength of Rock Mass (MPa)	Cohesion of Rock Mass (MPa)	Angle of Friction Rock Mass (Deg)
Weathered Serpentine	1840.107	0.138	2745.0	11.525	3.00	35
Serpentine	4064.160	0.138	2745.0	3.924	1.25	25
Chromite	6816.800	0.144	3537.9	3.570	1.25	20
Quartzite	5090.627	0.150	2350.0	17.156	4.00	40
Pyroxenite	1717.700	0.200	3000.0	11.939	4.18	20

Loading and Boundary Conditions

To apply loads, the models are constrained from two sides, those are (i) perpendicular to the strike of ore body and (ii) bottom surface. Surface traction pressure is applied to another side as shown in Figure 3b. The following equation is used for calculation of horizontal stress in finite element model according to depth of the ore body.

$$\sigma_h = 1.5 \times \sigma_v \quad \dots(4)$$

Where, σ_h : Horizontal stress perpendicular to the strike of the ore body (MPa), σ_v : Vertical stress (MPa)

Results and Discussions

All 2D finite element models have been analyzed using elasto-plastic behaviour of rock materials in plain strain condition. Results are enumerated in terms of principal stress distribution and plastic strains around the excavations.

Major Principal Stress (σ_1) Distribution

The major principal stress distribution around the stope and the decline is shown in Figure 4a. It is found that high stress concentration occurs at the corners of the stope.

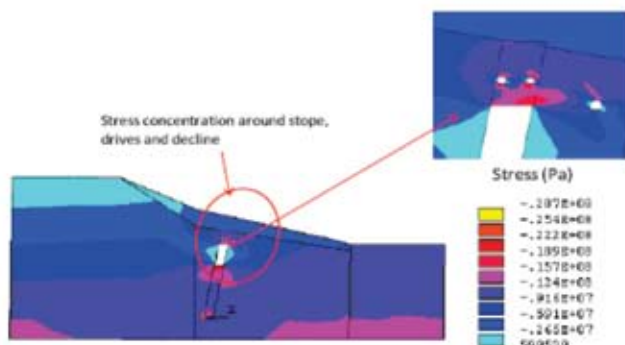
The peak major principal stress may range in between 15.7 MPa and 22.2 MPa. Tensile stress may develop in the hanging wall and foot wall rock masses.

Minor Principal Stress (σ_3) Distribution

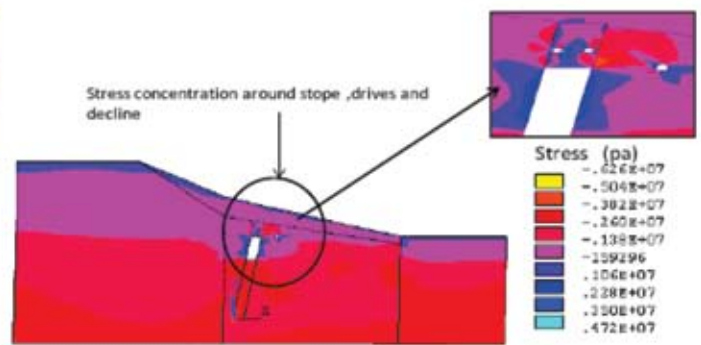
Distribution of minor principal stresses around the stope and the decline is plotted in Figure 4b. Tensile stress develops in the hanging wall, foot wall and the surrounding of the drives and also on the surrounding of the decline. Tensile stress ranges in between 2.28 MPa and 5.04 MPa depending on the location. This phenomena will cause plastic strains (yield zone) around the excavation.

The Plastic Zone

As mentioned earlier, the 2D vertical section has been analyzed to determine the plastic zone in the rock mass surrounding the decline. Figure 5 shows the intensity of plastic strains that has developed around the decline. In this case, a higher value indicates more failure of rock mass. These results clearly signify that proper support system is required to protect decline roof and side walls. The results also imply that a few locations, the crown pillar may yield and hence it requires reinforcement.



4a: Major Principal stresses of vertical section



4b: Minor Principal stresses of vertical section

Fig. : 4a and 4b

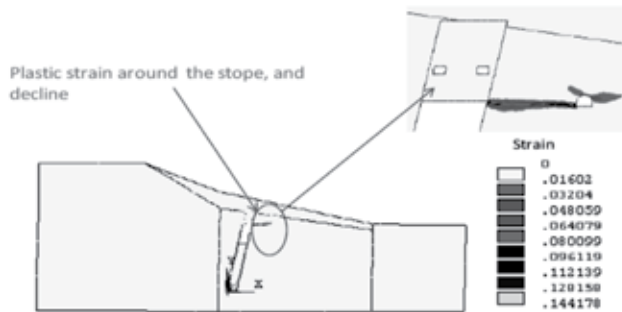


Fig. 5 : Distribution of intensity of plastic strain

Finite Element Models - 2D (Horizontal Section)

Horizontal Section Comprising Host Rock, Orebody and the Shaft

This model is developed to determine the plastic zone around the shaft area. The horizontal section has been taken at 155 mRL. This section is comprised of the shaft, plan section of rib pillars; excavations and host rock mass (Figure 6). It may be noted that authors have no intention to analyze stresses or displacements developed in this model. They are mainly interested to observe the failure zone surrounding the shaft and determine the strength properties of lining material based on that.

Generation of Finite Element Meshed Model

This 2D model has 1,355 six-noded triangular elements and around 2,872 nodes. Figure 6a shows the horizontal section of meshed model of ore-body and its surrounding areas. In general, finer mesh is developed around the stope and shaft zones. Coarser mesh is developed in the rock-body away from the mining-affected zones (zone of no-rock movement due to mining).

Loading and Boundary Conditions

The model is constrained from two sides, (i) along the strike of the ore body, and (ii) perpendicular to the strike of the orebody. Surface traction pressure is applied

from other two sides. The following equation is used for calculation of horizontal stress at a depth of 155 mRL.

Horizontal stress along the strike of the ore body,
 $\sigma_u = \sigma_v$, MPa ... (5)

Horizontal stress perpendicular to the strike of the ore body, $\sigma_h = 1.5 \times \sigma_v$, MPa ... (6)

Results and Discussions

The model is analyzed considering Drucker-Prager yield criterion in plane strain conditions. Material properties mentioned in Table 3 are also applied for this model. Results in terms of plastic zone around the shaft area are analyzed and presented below.

Distribution of Plastic Strain

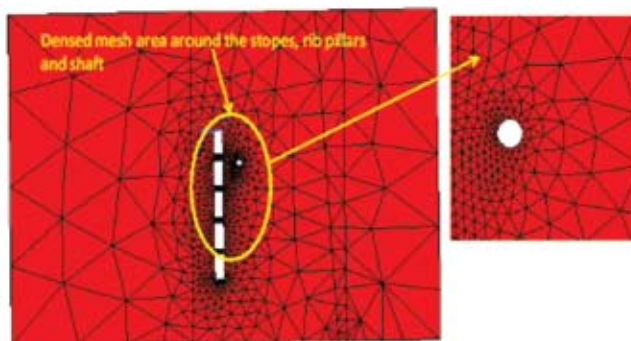
It can be observed that two corners of the model may experience failure due to shear (Figure 7). The intensity of plastic strain varies between 0 and 0.003165. Here, a higher value indicates severe failure of rock mass. This result signifies that concrete lining around the shaft is absolutely necessary. The following section deals with estimation of concrete strength of lining considering 0.3 m of lining thickness.

Strength of Lining Material

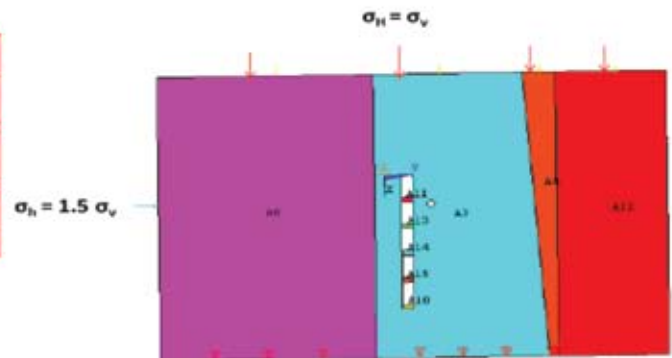
As mentioned before, biaxial far field stresses are applied in the finite element model. Due to this reason, non-uniform plastic zone has been developed around the shaft boundary as shown before. The critical radial pressure at various locations on the elasto-plastic boundary has been estimated as shown schematically in Figure 8. From stresses obtained in Euclidian plane, i.e., and are transformed into polar coordinates to calculate P_{cr} at different locations using the following stress transformation equations:

$$P_{\sigma} = \left(\frac{\sigma_{xx} + \sigma_{yy}}{2} \right) + \left(\frac{\sigma_{xx} - \sigma_{yy}}{2} \right) \cos 2\theta + \tau_{xy} \sin 2\theta \quad \dots (7)$$

$$\sigma_{cc} = \frac{(2 \times SF \times P_{\sigma})(a+t)^2}{(a+t)^2 - a^2} \quad \dots (8)$$



6a: Finite element mesh model



6b: Boundary condition is applied

Fig. : 6a and 6b

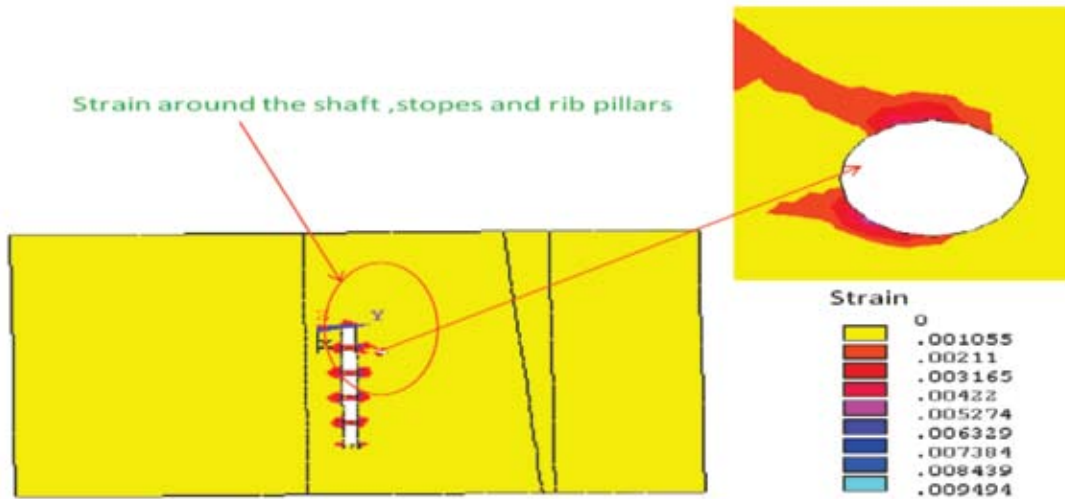


Fig. 7 : Distribution of intensity of plastic strain of horizontal section model

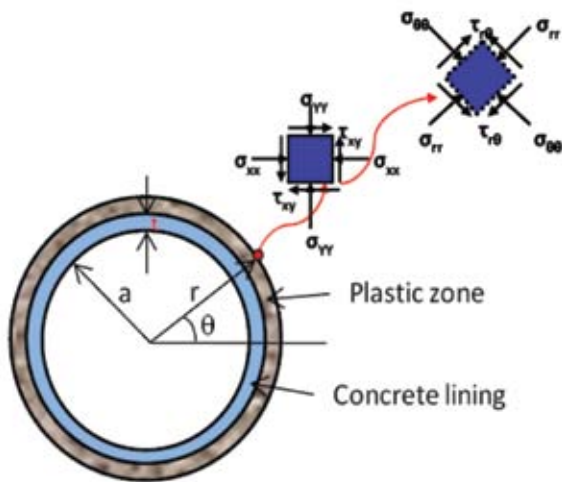


Fig. 8 : Schematic diagram of the critical radial pressure estimation.

where, σ_{cc} = Uniaxial compressive strength of concrete or shotcrete, SF = Factor of safety, t = Lining thickness, a = Finished radius of shaft.

The maximum value of the radial pressure is then taken as the critical pressure (P_{cr}) that may be considered for calculation of thickness or strength of lining material. Using the critical pressure value (P_{cr}), the required strength of the concrete lining of standard thickness of 0.3 m is calculated based on equation 9 (Brady and Brown, 2007). Table 4 lists the required compressive strength of the lining material for 0.3 m lining thickness having a safety factor of 1.5. It is found that compressive strength of concrete lining may vary from 16–48 MPa depending on the location. It is then recommended that on an average, the concrete strength for 0.3 m lining would be around 35–40 MPa. For this calculation, the elastic modulus of concrete is assumed to be 30 GPa.

Table 4 : Strengths of Lining of 0.3 m (SF = 1.5) in different locations

σ_{xx} MPa	-1.64	-2.3	-3.33	-4.32	-4.81	-5.63	-1.22	-1.46	-2.73	-1.13	-1.3
σ_{yy} MPa	-7.37	-7.98	-2.67	-7.05	-3.74	-2.82	-6.22	-8.94	-9.05	-7.83	-8.27
τ_{xy} MPa	0.13	-1.84	-2.51	-3.47	-3.5	-3.33	2.13	1.42	-0.51	1.58	1.44
P_{cr} MPa	1.71	1.81	0.94	2.65	1.71	0.98	1.16	1.62	2.79	2.2	2.68
σ_{cc} MPa	29.55	31.28	16.19	45.79	29.5	16.92	20.08	27.98	48.23	38.01	46.33

CONCLUSIONS

1. From 2D finite element analysis, it is found that failure zone may occur in the rock mass surrounding the unlined shaft, decline area and some part of the

stopes. To minimize this effect, concrete lining is required around the shaft boundary. In this study, 0.3 m lining is required with a reinforced concrete having a compressive of at least 35–40 MPa.

2. The permanent lining of the decline is composed of reinforced concrete beam of 1m width and an I-beam of 20 mm made of steel is placed in between 2 concrete beams. Prior to erection of the permanent lining, the ground is stabilized by grouted fore-poling method. Ribbed steel rods of 38 mm diameter and 3 m in length are grouted longitudinally across into the roof with a spacing of about 200 mm. These grouted bolts are welded into the nearest I-beam. If required, a steel plate is also placed over the grouted bolts to arrest the fall of loose soil or rock material, if any.
3. It is recommended that a composite support consisting of a 20 mm thick steel beam and 0.5 m wide reinforced concrete beam placed on either side of the steel beam is considered to represent one set of permanent lining of the decline. This dimension and configuration as mentioned above is considered to be adequate for the current analysis, since the 1 m wide concrete lining coupled with a 0.2 m wide steel I-beam placed at half way in the width are repeated as permanent lining throughout entire length of the lined part of the decline.

REFERENCES

1. Deb D, Mukhopadhyay S.K. and Suman R. 2007, "Efficacy of Numerical Analysis on Stability of Stope applying Three Dimensional Finite Element Method for a chromite ore body", Journal of the Mining, Geological & Metallurgical Institute of India, vol. 103, pp.83-93.
2. Gioda, G. and Swoboda, G., 1999, "Developments and applications of the Numerical Analysis of Tunnels in Continuous Media"; International Journal for Numerical and Analytical Methods in Geomechanics, pp. 1-2.
3. Brady B.H.G. and E.T. Brown, 2007, "Rock Mechanics for Underground Mining", Third Edition, Springer publication, pp. 577.
4. Kot F. Unrug, 1984, "Shaft design criteria", University of Kentucky, Lexington, Kentucky 40506 0046, USA, International Journal of Mining Engineering, pp 1-12.
5. Martin, C.D. and Maybee, W.G., 2000, "The Strength of Hard Rock Pillars"; International Journal of Rock Mechanics and Mining Sciences, pp.1239-1246.
6. Agustawijaya, D.S., 2006, "The Uniaxial Compressive Strength of Soft Rock"; International Journal of Rock Mechanics and Mining Sciences, pp.241-246.
7. Isadore Irvin Matunhire, 2007, "Design of Mine Shafts", Department of Mining Engineering, University of Pretoria, Pretoria, South Africa, pp 1-11.

BIOGRAPHICAL DETAILS OF THE AUTHORS

Islavath Sreenivasa Rao graduated in Mining Engineering from the University College of Engineering, Kakatiya University, Telangana in 2009. He obtained M Tech in Mining Engineering from Indian Institute of Technology, Kharagpur, India in 2012. He worked as Mining Engineer in Bharat Aluminium Company Ltd (BALCO) from 2009 to 2010. In June, 2012, he joined M/s Singareni Collieries Company Ltd (SCCL), Telangana as Mining Graduate Trainee. From October, 2013, he has been Assistant Professor in Mining Engineering at the University College of Engineering, Kakatiya University, Telangana. His specialization in rock mechanics, coal mining methods and numerical modelling.

Debasis Deb is a Professor of the Department of Mining Engineering at Indian Institute of Technology (IIT) Kharagpur, India. He holds BTech (Hons.) in Mining Engineering from IIT Kharagpur. He received his MS and PhD degrees in Mineral Engineering and Interdisciplinary Mining and Engineering Mechanics from the University of Alabama, Tuscaloosa, USA.

Sujeet Bharti is currently a Research Scholar of the Department of Mining Engineering, IIT Kharagpur and obtained an M.Tech. degree from the same department. He is a recipient of MHRD scholarship during his postgraduate degree. He graduated in Mining Engineering discipline from Institution of Engineers (India) in the year 2011. He won the Institution Prize from Institution of Engineers (India) in graduation. He is an Associate Member of Institution of Engineers (India). He is also a Life Member of MGMI and MEAI. He has been given title of a Chartered Engineer (India) from Institution of Engineers (India). He has more ten years experiences in rock testing, analysis and numerical modelling in ISM Dhanbad and IIT Kharagpur.